

Historic, Archive Document

Do not assume content reflects current scientific knowledge, policies, or practices.

A99.9
F7632U

C2



United States
Department of
Agriculture

Forest Service

Rocky Mountain
Forest and Range
Experiment Station

Fort Collins,
Colorado 80526

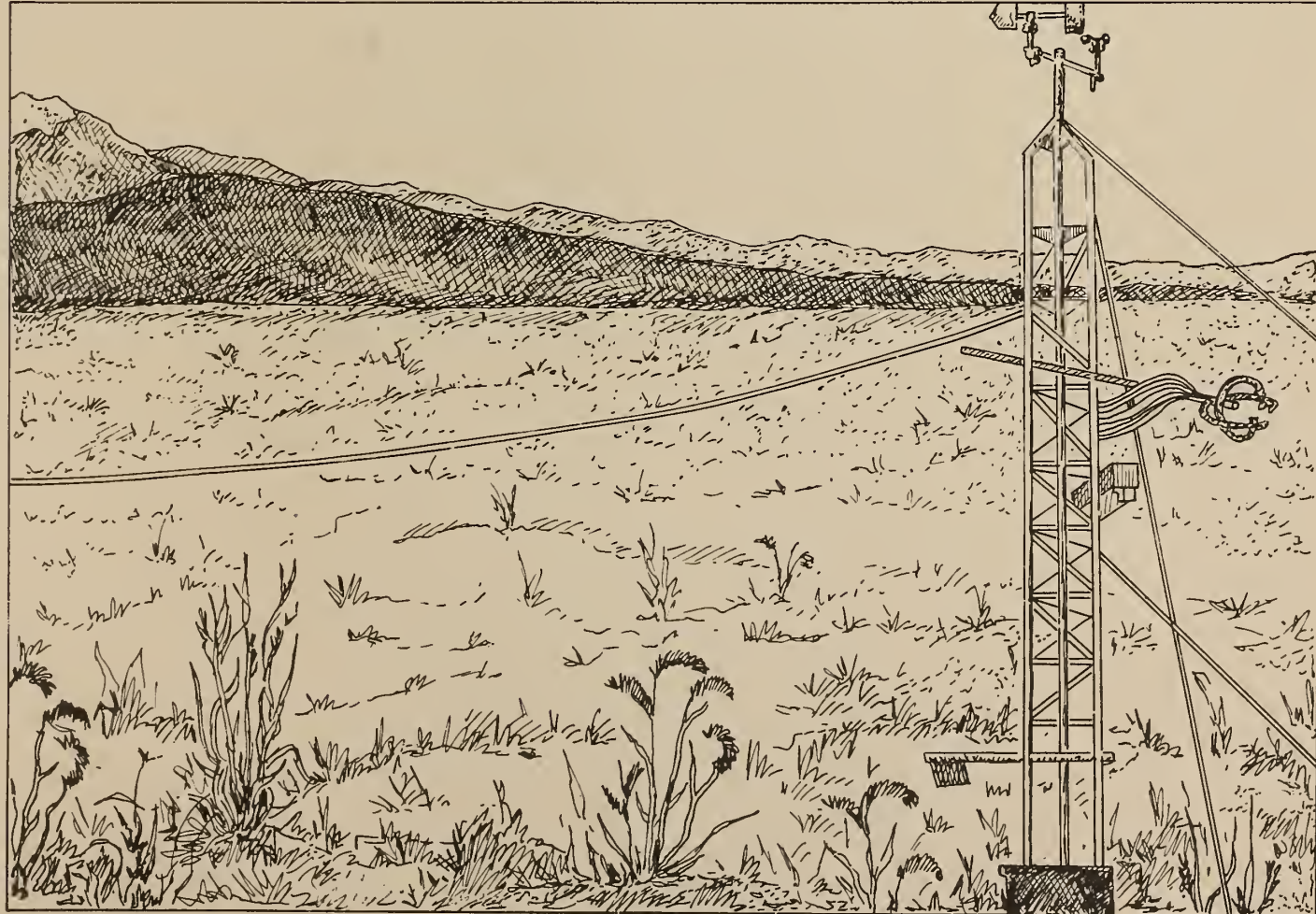
Research Paper
RM-288



Verifying Eddy Correlation Measurements of Dry Deposition: A Study of the Energy Balance Components of the Pawnee Grasslands

W. J. Massman
D. G. Fox
K. F. Zeller
D. Lukens

U.S. FOREST SERVICE
RECORDS
CO. / SERIALS BRANCH
JUN 1973



Abstract

The surface energy balance is used to assess the performance of the Pawnee Grasslands eddy correlation system. The four major components of the energy balance were measured: the net radiation, R_n ; the soil heat flux, G ; and the sensible and latent heat fluxes, H and λE , respectively. The latter two components of the energy balance were measured by eddy correlation. The surface energy balance defined as, $R_n - G = H + \lambda E$, was not achieved, most likely because measurements of R_n and G were not adequate.

Acknowledgments

The authors are indebted to Drs. H. Weaver, B. Tanner, E. Kanemasu, and B. Baker, and to Mr. P. Conklin for several helpful discussions. We also extend our thanks to Dr. D. Hazlett and Ms. D. Deutsch for their assistance in obtaining the CPER/LTER data.

Verifying Eddy Correlation Measurements of Dry Deposition: A Study of the Energy Balance Components of the Pawnee Grasslands

W. J. Massman, Meteorologist

D. G. Fox, Meteorologist

K. F. Zeller, Meteorologist

and

D. Lukens, Meteorological Technician

Rocky Mountain Forest and Range Experiment Station¹

¹*Headquarters is in Fort Collins, in cooperation with Colorado State University.*

Contents

	Page
Management Implications	1
Introduction	1
Instrumentation and Sources of Errors	2
Eddy Correlation Measurements	2
Net Radiation and Soil Heat Flux Measurements	5
Analysis of Data and Results	5
Conclusions and Recommendations	10
Literature Cited	10
Appendix A. Sonic Anemometer Shadowing Algorithm	12
Appendix B. Correction of Krypton Hygrometer for O ₂ Effect	13
Appendix C. Transfer Function for Krypton Hygrometer	13
Appendix D. A Digital Anti-Aliasing Filter	14

Verifying Eddy Correlation Measurements of Dry Deposition: A Study of the Energy Balance Components of the Pawnee Grasslands

W. J. Massman, D. G. Fox, K. F. Zeller, and D. Lukens

Management Implications

The health and productivity of any ecosystem are dependent upon how that ecosystem utilizes energy. In order to predict how ecosystems are likely to respond to changes in climate or concentrations of atmospheric pollutants (e.g., SO_x , NO_x , O_3), it is necessary to understand how energy is transformed and used as it flows through the ecosystem. The first step toward achieving this understanding is the quantification of the major components of the surface energy balance.

At the Central Plains Experimental Range/Long-Term Ecological Research (CPER/LTER) site at the Pawnee National Grasslands, scientists from both the Rocky Mountain Station and the Natural Resources Ecology Laboratory of Colorado State University are independently attempting to measure several major components of the surface energy balance. This report describes how well independent measurements of radiation and the transport of heat and water vapor achieve closure of the surface energy balance and, thereby, account for the gross energy available to and processed by an ecosystem. The motivation behind this study is to evaluate the eddy correlation technology which we have been using to measure the exchange of gaseous pollutants (NO_2 , NO_x , and O_3) between the atmosphere and the grassland ecosystem (Zeller et al. 1989).

Eventually, we plan to make eddy correlation measurements over sensitive forested alpine and subalpine ecosystems and to use this measurement approach to confirm simpler technologies for routine measurements of the levels of ozone, sulphur, and nitrogen present and depositing to forested lands.

Introduction

In a previous paper (Zeller et al. 1989), we detailed a dry deposition measurement program that uses an eddy correlation system to measure the fluxes of ozone, NO_2 , and NO_x at the Pawnee National Grasslands. In that report we emphasized sources of errors associated with the eddy correlation method and outlined procedures to correct those errors in subsequent data analysis. In this paper we use constraints placed on the eddy correlation system by the balance of energy flowing into and away from the surface to further assess the validity of eddy correlation technology. In general, the surface energy balance is a good, but not necessarily an absolute, check on the eddy correlation method.

The surface energy balance over an ecosystem quantifies how radiant energy input into that system is divided

into various components and utilized by that ecosystem. For example, a general surface energy balance can be written as follows:

$$R_n = G + H + \lambda E + P + S + D \quad [1]$$

where R_n denotes the net radiation and represents the difference between the total incoming radiation (mostly direct and diffused solar radiation) and the outgoing radiation (mostly reflected incoming radiation and terrestrial longwave radiation); G is the soil heat flux; H is the vertical component of the sensible heat flux; λE is the vertical component of the latent heat flux (the evapotranspiration rate or moisture flux, E , multiplied by the latent heat of vaporization of water, λ); P is the energy required for photosynthesis; S is the heat energy stored in the biomass and inside the canopy airspace of the surface plant cover; and D is the horizontal component of sensible and latent heat fluxes.

At Pawnee, as is the case in general, the energy balance is dominated by four major components: R_n , G , H , and λE . Of the other three components, P and S are insignificant at Pawnee. For example, P at Pawnee is between 0.25% and 2.0% of solar radiation (Brown and Trlica 1977) or between 2.5 watts per square meter (wm^{-2}) and 20 wm^{-2} with a nominal value of about 5 wm^{-2} at our site under normal soil moisture conditions. While the energy storage component, S , can be significant for forested ecosystems (McCaughey and Saxton 1988, Moore 1986a), it is unlikely to be even as large as P for our site because the plant cover is fairly dry, herbaceous, and short (maximum plant height about 25 cm) and covers at most no more than half the surface (Brown and Trlica 1977). The horizontal component, D , on the other hand, may contribute significantly under some circumstances. But, because the technology to conveniently evaluate D does not exist, most eddy correlation experiments are performed over relatively flat, homogeneous surfaces, where D can be assumed to be small. Although we are unable to directly measure this component, we can, for particular wind directions, infer its contribution to the energy balance. As discussed in a later section, this will provide an estimate for an upper limit on the magnitude of D .

Therefore, for the purposes of this work, the relationship between R_n , G , H , and λE is expressed in the energy balance equation and is given as follows:

$$R_n - G = H + \lambda E \quad [2]$$

This expression forms the basis for assessing the performance of the eddy correlation system at the Pawnee Grasslands. Specifically, we determine H and λE by eddy correlation and independently determine R_n and G using

a net radiometer and a soil heat flux plate, respectively. Therefore, the degree of closure of equation [2] should permit us to evaluate how well the eddy correlation system performs.

The intent of this paper is to detail our efforts at closing equation [2] and to present a further assessment of the Pawnee eddy correlation system for dry deposition. We first describe, in a manner which is consistent with Zeller et al. (1989), the instrumentation employed for this study and then we present the results of our data analysis. For a description of the Pawnee site and a discussion of the general nature of eddy correlation systems, and our specific implementation of it, the reader is referred to Zeller et al. (1989).

Instrumentation and Sources of Errors

Eddy Correlation Measurements

We begin this section with a brief discussion and definition of the eddy correlation method and how it is employed to determine the sensible and latent heat fluxes. As discussed by Zeller et al. (1989), eddy correlation is an aerodynamic method for directly estimating the vertical flux of a quantity to or from an underlying surface. In essence, this method determines (at a level several meters above the surface) the covariance between the fluctuations in the vertical velocity and the fluctuations in the concentration of that quantity. However, in order for these flux measurements to be representative of the surface fluxes, we must assume that there are no physical processes between the surface and the level of observation that could significantly interfere with or distort the surface fluxes. In general this is true, but not always. One situation where this assumption may fail is whenever small patches of the surface are heated or cooled differently from their surroundings. When this occurs, the horizontal flux term, D , of equation [1] can contribute significantly to the energy balance. As will be discussed in the next section, D may continually be influencing the eddy correlation measurements at our site.

The eddy correlation system discussed in this report directly measures the fluxes of temperature and water vapor denoted by $w'T'$ and $\rho_v'w'$, respectively. Here w' is the fluctuation in the vertical velocity measured after correcting the velocity to have no mean vertical component, T' is the fluctuation in the atmospheric temperature after the removal of the mean ambient temperature, and ρ_v' is the fluctuation in the water vapor density also after the removal of the mean ambient vapor density. The overbar refers to the covariance between the two quantities. From the covariance measurements we determine the sensible and latent heat fluxes. The sensible heat flux (in wm^{-2}) is $\rho c_p w' \theta'$ and the latent heat flux (also in wm^{-2}) is $\lambda \rho_v' w'$, where ρ is the mass density of the atmosphere ($\rho = 1.0 \text{ kgm}^{-3}$ for our site), c_p is the specific heat capacity of air at constant pressure ($c_p = 1005 \text{ jkg}^{-1} \text{ K}^{-1}$), θ' is the fluctuation in potential temperature ($\theta' = 1.05T'$ for our site which has an elevation of 1641 m and a mean ambient atmospheric pressure of 85 kPascals),

and λ is the latent heat of vaporization for water and is given as follows:

$$\lambda = 1.91846(T_0/(T_0 - 33.91))^2 \text{ (MJ kg}^{-1}\text{)}$$

where T_0 is the temperature of the evapotranspiring surface in degrees K (Henderson-Sellers 1984).

For measurements of w' and T' we use, respectively, a 3-axis sonic anemometer and a fast response platinum wire resistance thermometer (Zeller et al. 1989). For measuring ρ_v' we use a fast response krypton hygrometer which was added to our eddy correlation system on May 26, 1988, subsequent to the time period discussed in Zeller et al. (1989). Table 1 provides more detailed information on these and all other instruments used in this study. All real time data collection, processing, and computations are discussed by Zeller et al. (1989). Once the data are taken and stored, they are transferred to a mainframe computer at Rocky Mountain Station for further analysis.

As discussed in Zeller et al. (1989), eddy correlation data are subject to several different types of corrections. In this report we discuss corrections for $\overline{\rho_v'w'}$ and for the sonic anemometer data which were not covered in Zeller et al. (1989). Four important corrections are considered herein. The first is the shadowing effects of the sonic anemometer (Conklin et al. 1988), the second is the influence O_2 has upon the krypton hygrometer (Tanner and Greene 1989), the third involves the sensor inadequacies associated with spatial averaging effects of the krypton hygrometer (Andreas 1981) and the distance separating the sonic anemometer and the krypton hygrometer (Moore 1986b, Zeller et al. 1989), and the fourth is the correction due to atmospheric density fluctuations associated with heat and moisture fluxes (Webb et al. 1980).

Shadowing effects.—Shadowing effects arise due to the blocking of the wind by the wind-sensing transducers themselves. To correct for shadowing effects, we used wind tunnel data provided by Conklin (1988) to develop an algorithm detailed in appendix A which is applied in real time sensor output. The results show that uncorrected estimates of $w'T'$, $\rho_v'w'$, or any other scalar fluxes are underestimated by about 16% because of shadowing.

Oxygen influence.—The presence of atmospheric oxygen influences the measurement of latent heat flux by the krypton hygrometer (Tanner and Green 1989). Using data supplied by Tanner² we developed the following correction for this effect:

$$\overline{\rho_v'w'} = (\overline{\rho_v'w'})_m + (\alpha \overline{w'T'})/T \quad [3]$$

where the subscript m refers to the measured quantity, α is a constant ($\alpha = 0.0131 \text{ kgm}^{-3} \pm 0.0018 \text{ kgm}^{-3}$), T is the ambient atmospheric temperature in degrees K, and $w'T'$ is expressed in ms^{-1}K . The correction given by equation [3] was applied after the raw data had been transferred to the mainframe; however, it could also be applied in real time. This relationship is useful for correcting fluxes derived from the krypton hygrometer, but not for estimates of the variance of the water vapor den-

²Tanner 1989 – personal communication.

Table 1.—Instrumentation used for the surface energy balance study at the Pawnee Grasslands Acid Deposition Research Site.¹

Type of instrument	Manufacturer	Comments
3-axis sonic anemometer	Atmospheric Technologies, Inc.	rotated position
Fast response krypton hygrometer	Campbell Scientific KH20	
Fast response platinum wire thermometer	AIR, Inc.	
Net radiometer	Radiation Energy Balance Systems (Q*4)	double dome Fritsch type operational after 6/27/88
Soil heat flux plate	Radiation Energy Balance Systems	10 cm depth operational after 6/27/88
Net radiometer		CPER/LTER single dome Fritsch type new calibration 8/15/88
Soil heat flux plate	Qualimetrics Heat flow sensor # 3983	CPER/LTER 1 cm depth
Temperature probe	Fenwal Electronics thermistor UUT51J1	CPER/LTER
Relative humidity	LiCl cell Phys-Chemical Research PCRC-11 RH sensor	CPER/LTER

¹The use of trade and company names is for the benefit of the reader; such use does not constitute an official endorsement of approval of any service or product by the U.S. Department of Agriculture to the exclusion of others that may be suitable.

sity. Another approach is required for correcting the variance estimates. More details about this correction are given in appendix B.

Spatial averaging effects.—Inadequate sensor response characteristics can also cause significant underestimations in the flux and variances measurements provided by eddy correlation. Both Zeller et al. (1989) and Moore (1986b) discuss these at length. Corrections for $w'T'$ are detailed in Zeller et al. (1989), and appendix C provides the background for similar corrections to $\rho_v'w'$. The results of appendix C provide figures 1 and 2 which give, respectively, the percent underestimation in the flux and variances measurements taken with the krypton hygrometer. From these figures we see that $\rho_v'w'$ will be underestimated, depending upon atmospheric stability, by about 15% to 20% at our site where the mean horizontal wind speed is usually in excess of

1 ms^{-1} . Corrections for these effects are applied after the raw data have been transferred to the mainframe.

Atmospheric density variations.—Another correction for vapor flux measurements is discussed by Webb et al. (1980) and arises because of atmospheric density fluctuations primarily associated with the heat flux and secondarily with the moisture flux. Due to the relatively low humidity and generally low evapotranspiration rates (moisture flux) at our site, it is sufficient to consider corrections due to the heat flux only. With this simplification this last correction can be expressed in a form similar to equation [3] above:

$$\overline{\rho_v'w'} = (\overline{\rho_v'w'})_m + (\rho_v w' T')/T \quad [4]$$

where ρ_v is the mean ambient concentration of water vapor. For our site this correction and that given by equation [3] can be significant sometimes totaling more than

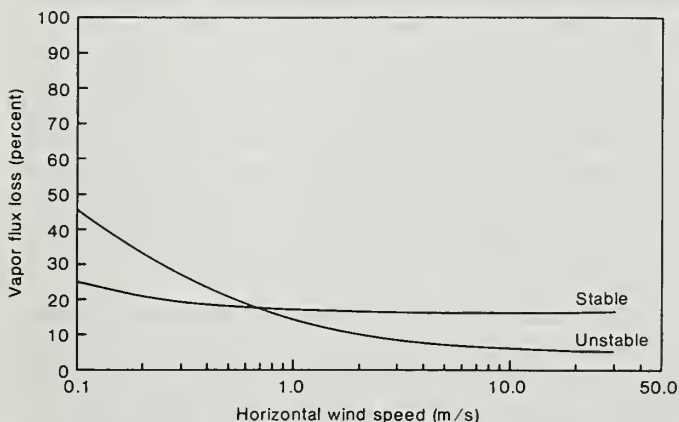


Figure 1.—Estimates of latent heat flux loss as a function of wind speed and atmospheric stability for the krypton hygrometer and a 3-axis sonic anemometer.

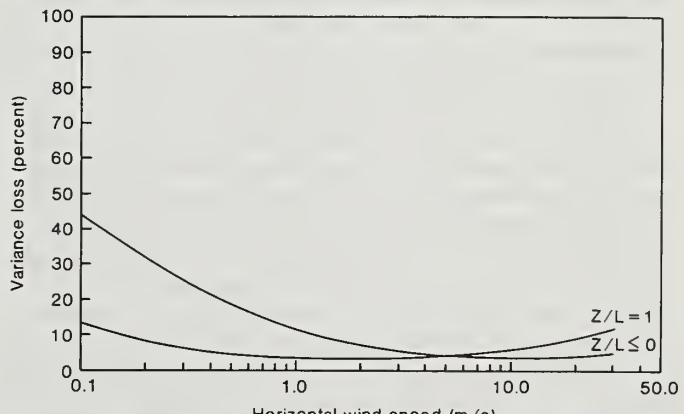


Figure 2.—Estimates of vapor density variance loss with krypton hygrometer as a function of wind speed and atmospheric stability.

20%. However, the mean vapor density at the Pawnee Grasslands rarely exceeds 0.01 kg m^{-3} , and typically is about 0.005 kg m^{-3} ; hence, the correction for oxygen, equation [3], is usually the major correction. Equation [3] provides for a correction usually between 6% and 12% to $(\bar{\rho}_v' w)_m$ while equation [4] typically accounts for another 3% to 8% correction.

In addition to the above four corrections, another important aspect of eddy correlation is the problem of aliasing. Aliasing results whenever any continuous variable is sampled at discrete intervals and in general causes the flux or variance to be overestimated. If only naturally occurring atmospheric frequencies are aliased, then the flux or variance of that quantity will be in error by no more than 2% or 3% for sampling frequencies appropriate to eddy correlation (i.e., 10 Hz or above). However, when data are collected with electronically noisy instruments, aliasing can cause more significant errors. Fortunately, anti-aliasing filters can largely eliminate the errors associated with aliasing (Kaimal et al. 1968). Appendix D discusses the design of a digital version of an anti-aliasing filter known as a Butterworth filter. Since this filter was not installed in the data gathering system by the time of this report, the data discussed herein (as well as in Zeller et al. 1989)³ do suffer from aliasing. For Zeller et al. (1989), this was only a minor problem with the temperature sensor. For the present report, the anemometer, the hygrometer, and the temperature sensor are all aliased. However, aliasing is not expected to cause more than a 3% error to the flux measurements, or to impact the results of the present paper or of its predecessor (Zeller et al. 1989). Once the filter outlined in appendix D is implemented, aliasing should cease to be of any concern at all.

Up to this point we have discussed matters pertaining only to the fluctuating quantities T' and ρ_v' . However, the expression for λ suggests that T_0 needs to be considered and equations [3] and [4] clearly indicate that reliable measurements of the mean quantities T and ρ_v are also needed. We do not measure T_0 , but fortunately the heat of vaporization, λ , is only weakly dependent upon T_0 within the temperature range encompassing our observations. For our purposes we will substitute T for T_0 in the expression for λ . This should cause no more than about a 1.5% error in the measured values of λE , which is somewhat less than the error which would be introduced by using a constant value for λ (Henderson-Sellers 1984).

Measurements of T and ρ_v were taken with the platinum wire thermometer and the krypton hygrometer, respectively. Generally, the use of these fast response sensors to determine absolute measurements of ambient vapor density and temperature is not recommended because they are poor devices for making absolute measurements. However, our experience suggests that with care they can in fact be used for estimating T and ρ_v when computing the corrections outlined in equations [3] and [4]. The uncertainty in the flux measurements introduced with this approach for our site is no more than about 5% and most commonly will be less than 3%,

³Zeller et al. (1989) briefly discuss aliasing but they did not detail their efforts at eliminating it.

even though the absolute measurements may be significantly in error. The flux measurements are relatively insensitive to these errors because the temperature is expressed in degrees K and, therefore, a few degrees inaccuracy will not produce significant errors, and, because the Pawnee Grassland site is generally quite dry so that the vapor density ρ_v is generally quite low and, hence, will not contribute very much to equation [3]. Furthermore, we also compared data from the fast response sensors with similar data taken at the nearby CPER/LTER site (which is separated from ours by about 40 m). Table 1 provides more details on the CPER/LTER sensors.

Our temperature sensor generally agreed with the CPER/LTER thermistor to within 15°C, with the greatest differences between the two sensors usually occurring at night. The CPER/LTER thermistor, which is located about 2 m above the surface, consistently read colder at night than did our fast response temperature sensor, positioned 6 m or 8 m above the surface. Stable stratification of the atmosphere and the relative vertical placement of the two sensors account for much of their observed nighttime differences. During the day, these two sensors usually agreed to within 10°C and frequently were much closer. Only during one 4-day period did the fast response temperature sensor exhibit any calibration drift relative to the CPER/LTER thermistor, and we corrected the fast response sensor by adding a +11°C offset. In addition to this comparison, we also recalibrated our fast response temperature sensor weekly with a separate hand-held temperature sensor.

Our krypton hygrometer generally agreed to within a factor of two with the CPER/LTER LiCl humidity probe, and both instruments showed that ρ_v rarely exceeded 0.01 kg m^{-3} and commonly was between 0.002 and 0.006 kg m^{-3} . Again, the discrepancy between these two sensors is not important for making the corrections above. However, this comparison did allow us to identify and correct a shift in the calibration of the krypton hygrometer which occurred whenever ρ_v fell below about 0.003 kg m^{-3} . Below this value of vapor density the nominal calibration curve for the krypton hygrometer is no longer valid and the krypton hygrometer can be seriously in error for both ρ_v and ρ_v' . In general this calibration shift was not a problem, except for 2 weeks at the end of our data gathering period. Based on a separate calibration curve for these 2 weeks derived from the original calibration curve, we recomputed ρ_v and reduced the vapor flux, $\bar{\rho}_v' w$ by 10%. About 3 months after this 2-week period, we had the original calibration curve rechecked and extended beyond its original lower limit of about 0.002 kg m^{-3} . This recalibration confirmed the assumptions we had made when deriving the new calibration curve from the original calibration curve.

In addition to this calibration shift at low humidities, the krypton hygrometer can also change calibration due to scaling of the source tube window. Tanner (1988) states that this can cause about an 8% error in the flux measurements. To minimize this error we cleaned the hygrometer window at least once a week and often more frequently. Our experience here suggests that our site

is relatively clean and, therefore, we do not expect scaling to be a major problem.

In summary, we believe that the sensible and latent heat fluxes derived from our eddy correlation data are accurate to within 5% to 10%, and we base this claim on the nature of the approximations and corrections we have outlined above. We also wish to emphasize that the preceding discussion of eddy correlation is so detailed because eddy correlation cannot be used without some understanding of its inherent limitations. On the other hand, we are encouraged by the ability to correct for instrument inadequacies as described above and in the appendices.

Net Radiation and Soil Heat Flux Measurements

The net radiation and soil heat flux are not measured by eddy correlation. For measuring net radiation, we use a double dome Fritschen-type net radiometer; for soil heat flux, we use a standard heat flux plate. These instruments were installed at our site on June 26, 1988. Table 1 provides the details of the sensors used for these measurements.

The net radiometer is pointed southward and is suspended from a 1-m-long metal pipe about 1.5 m above the Pawnee Grassland surface. The metal pipe is supported by a metal A-frame horse about 3 m long. This mounting was chosen to minimize the contamination of the radiometer signal by the mount itself. The horse is guyed by a wire to prevent it from moving in the wind. The soil heat flux plate is buried at a depth of 10 cm on the north side of a tuft of grass 2 m from one of the legs of the horse. It is positioned so that about half of the heat flux plate is directly beneath the tuft of grass and the remaining portion is beneath the bare soil surface. The horse is positioned about 8 m west and slightly north of the eddy correlation shelter and 20 m south and west of the meteorological tower on which the eddy correlation instruments are mounted. Zeller et al. (1989) give more details on the physical layout of the eddy correlation system. Data taken at the eddy correlation site is recorded once every half-hour. Net radiation and soil heat flux data are recorded once every half-hour on a Campbell Scientific CR-21x data logger⁴ and coincide with the eddy correlation measurements of heat and moisture fluxes.

In addition to our instrumentation, the nearby CPER/LTER site also includes a separate net radiometer and soil heat flux plate as well as a weighing lysimeter. These instruments, as discussed in the next section, provide separate estimates of R_n , G , and λE , which are compared to our data. The net radiometer is mounted on the CPER/LTER meteorological tower about 1.5 m above the surface and faces southward. The heat flux plate is buried beneath 1 cm of bare soil about 1 m south of the tower, and the weighing lysimeter is about 3 m north of the tower and was specifically designed and built for the

CPER/LTER site (Armijo et al. 1972). The net radiometer is a single dome Fritschen-type net radiometer. Table 1 gives more detail on these sensors. Data taken at the CPER/LTER site is recorded once every hour on a Campbell Scientific CR-21x data logger.

As with the eddy correlation instrumentation, these net radiometers and soil heat flux plates and the weighing lysimeter are all subject to specific errors as will be discussed in the next section. However, when we compare data from these different instruments it is important to keep in mind that each set of instruments is sensing a slightly different surface area. For example, the latent heat flux as measured by the lysimeter is representative of the surface of the soil core contained within the lysimeter; on the other hand, the eddy correlation system at a height of 8 m above the surface senses a much larger surface area than does the lysimeter. We can only assume that the flux data from either of these instruments is representative of the same Pawnee Grassland surface. Therefore, we may expect, *a priori*, some discrepancies not only in the evapotranspiration measurements but in the net radiometer measurements and the energy balance closure as well. Although our research does not directly address the question of surface area representation it is an important consideration and one which is relevant throughout this work.

Analysis of Data and Results

The data used in this study were collected from May 26, 1988, through October 30, 1988. As with all experiments of this type, the data needed to be edited. We identified 48 days during this 5-month period which potentially could be used to study the daily course of the surface energy balance at the Pawnee Grasslands. For our purposes 1 day of data is any 24-hour period during which the eddy correlation system had virtually a 100% data recovery rate. Of these 48 days, the 26 days used in this report were selected on the basis of wind direction and the quality of the data. (These data are virtually free of electronic noise.) Twenty days had favorable wind direction during which the wind was not blowing across the eddy correlation shelter and/or through the meteorological tower, and 6 days had extensive periods of time usually around noon during which the wind was blowing over the shelter and through the tower. In this report, such an unfavorable wind direction is between 195 degrees and 215 degrees. We include these last 6 days of data to document the influence of site geometry on the sensible and latent heat fluxes. The remaining 22 days not reported on here had a mixture of variable wind regimes, somewhat more noise, or a somewhat greater data dropout rate.

These 26 days of data are further divided into 2 different time periods. The first comprises 5 days of data taken between June 26 and July 23, and the second includes 21 days of data taken between September 14 and October 30. Originally only the first period had been planned; however, during this period the CPER/LTER net radiometer was not available for comparisons with our net radi-

⁴The use of trade and company names is for the benefit of the reader; such use does not constitute an official endorsement or approval of any service or product by the U.S. Department of Agriculture to the exclusion of others that may be suitable.

ometer, and since this comparison is central to the results of this report the second data period was necessary. But the specific dates defining the second data period were determined by other constraints. The eddy correlation system suffered virtually a complete loss of data between July 24 and September 16 for two independent reasons. First, for 2 weeks beginning on July 24 the system was undergoing a major reconfiguration of the sensors on the tower and, therefore, much of these data are probably untrustworthy. Second, on August 13 a fire damaged the interior of the eddy correlation shelter, destroying about 2 weeks of potentially useful data and causing a hiatus of almost 1 month in the data gathering effort.

Finally, each day was further classified as either wet or dry surface, depending on how soon after a rain the data were taken. Often the wet surface days include partial or variable cloud cover and, hence, in general tend to be somewhat cooler than the dry surface days. Here we use the descriptors wet or dry to refer to those times when the soil evaporation is or is not likely to be contributing significantly to the total surface evapotranspiration rate. Table 2 summarizes the dates and character of each of the 26 days used in this report.

We employ three methods for analyzing these 26 days of data: the 24-hour averaged energy balance ratio (EBR); the half-hourly energy difference (ED); and the direct comparisons between our estimates of the soil heat flux, the latent heat flux, and the net radiation and the estimates of each of the same quantities as derived from the CPER/LTER data. We begin by defining and discussing the results from the first of these approaches.

The EBR is defined as follows:

$$EBR = \frac{\sum(H + \lambda E)}{\sum(Rn - G)} \quad [5]$$

where the summation extends over 24 hours. By summing the energy balance components over a diurnal cycle, we should minimize or eliminate errors in G (since $\sum G \sim 0$) and any errors introduced by ignoring heat storage in the biomass. If closure were perfect equation [2] requires that EBR ~ 1 . From the results (table 2, fig. 3), however, we have not achieved closure since EBR ranges between about 0.60 and 0.82 for the days of favorable wind direction and even less for those days of unfavorable wind direction. Either the eddy correlation $\sum(H + \lambda E)$ is too low or the $\sum(Rn - G)$ is too high. We will show that the latter appears to explain the discrepancy.

Errors of this magnitude in the energy balance (200 Wm^{-2} to 300 Wm^{-2}) are not likely to be caused by underestimations in the latent and sensible heat fluxes especially after they have been as extensively corrected as described earlier for known deficiencies. We estimated the corrected eddy correlation measurements are not likely to be in error by more than 5% to 10%. Assuming a 10% underestimation in each of the half-hourly measurements of $w'T'$ and $\rho_v'w'$, recomputing the EBR for each of these 26 days resulted in individual ERBs that were about 10% above the values shown in figure 3. However, to achieve energy balance closure by assuming that the eddy correlation measurements are in error would require an additional underestimation of 20% to 40% of these energy fluxes which is not realistic. The results suggest other possibilities. The double dome net

Table 2.—Description of data set used for the surface energy balance study at the Pawnee Grasslands Acid Deposition Site.

Date 1988	Wind direction Favorable/unfavorable	Surface conditions		Sky conditions	EBR
		Wet/dry			
June 27	F	D		cloudy	0.77
July 1	F	D		clear	0.66
July 8	F	W		cloudy	0.78
July 9	F	W		cloudy	0.74
July 10	F	D		clear	0.60
September 14	U	W		cloudy	0.67
September 17	F	W		clear	0.72
September 19	F	D		clear	0.61
September 29	F	D		clear	0.75
September 30	F	D		clear	0.75
October 1	F	D		clear	0.66
October 2	U	D		clear	0.56
October 3	F	W		clear	0.73
October 4	F	W		mid-day clouds	0.82
October 8	F	W		clear	0.66
October 9	F	D		clear	0.70
October 10	F	D		clear	0.69
October 13	F	D		clear	0.66
October 15	F	D		clear	0.63
October 21	F	W		clear	0.62
October 23	U	D		cloudy	0.43
October 24	U	D		clear	0.55
October 26	U	D		clear	0.41
October 28	F	D		clear	0.65
October 29	U	D		cloudy	0.52
October 30	F	D		cloudy	0.62

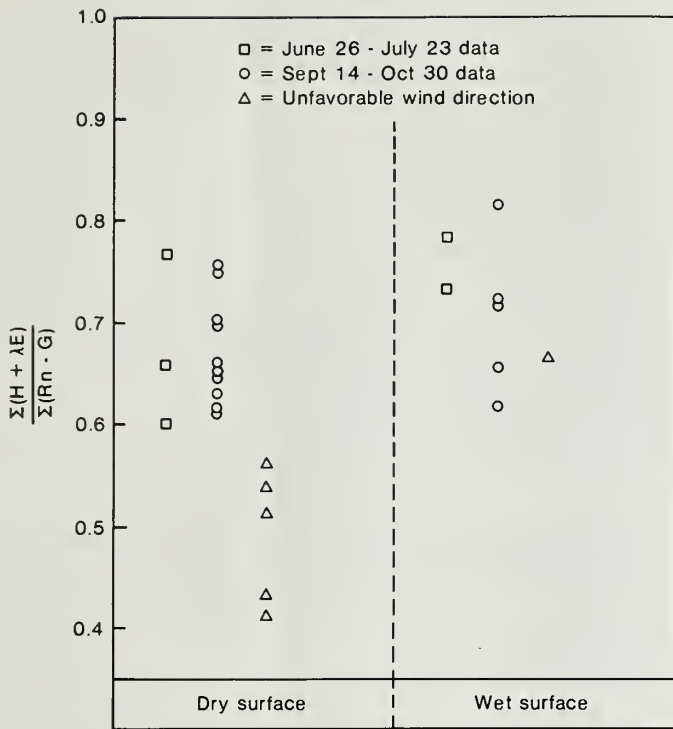


Figure 3.—Computed values of the EBR (equation [5] of text) for the 26 days listed in table 2.

radiometer used for the measurement of R_n may be underestimating the outgoing terrestrial long wave radiation and/or our site geometry (or horizontal effects) may significantly influence the flux measurements.

Undermeasurement by the net radiometer is supported by comparing days when the surface is wet and relatively cooler to those when it is dry and relatively warmer. During both data gathering periods there is a tendency to achieve a slightly better closure on days when the surface is wet and cooler than when it is dry. The average EBR for the 13 dry surface days is 0.67, whereas it is 0.72 for the 7 wet surface days, supporting this contention. However, other studies also suggest that this type of net radiometer underestimates the long wave component of the terrestrial radiation. Both Weeks et al. (1987) and Kanemasu⁵ reached this conclusion from separate and much more detailed studies of radiometer performances. Furthermore, Weeks et al. (1987) also reported EBR values at their site near Artesia, New Mexico that are quite similar to those given in table 2 and figure 3.

Horizontal effects influence the EBR on days when the surface conditions are dry and the wind direction is unfavorable. It is possible that large scale atmospheric effects could also be responsible for the EBR values; however, this seems unlikely. Since we defined unfavorable winds to be from the southwest, any large scale horizontal advective effects would likely cause a warming which would cause the eddy correlation system to overestimate the heat flux and consequently improve the energy balance closure. Rather, we believe that the poor closure during unfavorable wind directions and dry surface conditions is caused by cooling of the air as it passes

over the relatively cool, highly reflective, instrument shelter. On a day (9/14, table 2) with relatively cooler surface conditions and unfavorable winds the closure is much better, consistent with the expectation that a wet and relatively cool surface is less likely to exchange energy between the shelter and the ambient air passing over it. (We will discuss this contention in more detail later.) Energy differences between the favorable and unfavorable wind regimes on the days with dry surface conditions correspond to discrepancies of between 100 and 200 wm^{-3} in the energy balance, and they provide a good, albeit rather extreme, example of how significant the D component of the energy balance can be. In general, D will not cause such large imbalances because the shelter is a large and significant surface in homogeneity in the upwind direction. The magnitude of this error also provides an upper limit on the magnitude of D in equation [1].

The half-hour energy difference is defined as follows:

$$ED = R_n - G - H - \lambda E \quad [6]$$

Figure 4 gives the daily course of ED for the 10 dry soil days during the fall data gathering period and clearly illustrates the lack of energy balance closure. On this figure we have also plotted the mean difference and one standard deviation of the difference between the two net radiometers for the same time period. It is clear that the mean difference between radiometers is slightly less than what might be expected for the mean ED value. In other words, had we used the CPER/LTER radiometer, we would have come significantly closer to closure of the energy balance.

Figure 5 gives a comparison of the 24-hour time courses for the two net radiometers for September 19, 1988. This figure is an example of the general relative performance of the two net radiometers with the double dome radiometer reading higher most of the time. The next figure, figure 6, gives a more detailed comparison between the net radiometers. This figure gives the regression coefficient, a_r , for each 24-hour period for the fall data set for both day ($R_n > 0$) and night ($R_n < 0$) and wet and dry surface conditions. Here a_r is determined by a least squares method according to the following relationship:

$$(R_n)_{\text{single dome}} = a_r (R_n)_{\text{double dome}}$$

In general, the major differences in the relative performance of these sensors is between night and day and not between wet and dry surface conditions. Therefore, disregarding the wet versus dry distinction, the median value of a_r for night is 1.30, whereas for day it is 0.88 so that in general the double dome net radiometer tends to read higher than the single dome radiometer. These results are completely consistent with the contention that the double dome net radiometer is not sensing all of the outgoing longwave radiation. However, in addition to this linear regression test, we also considered a constant offset term (i.e., $(R_n)_{\text{single dome}} = a_r (R_n)_{\text{double dome}} + b_r$ and $(R_n)_{\text{single dome}} = (R_n)_{\text{double dome}} + b_r$), but the results did not indicate any possibility of a constant

⁵Kanemasu 1988 – personal communication.

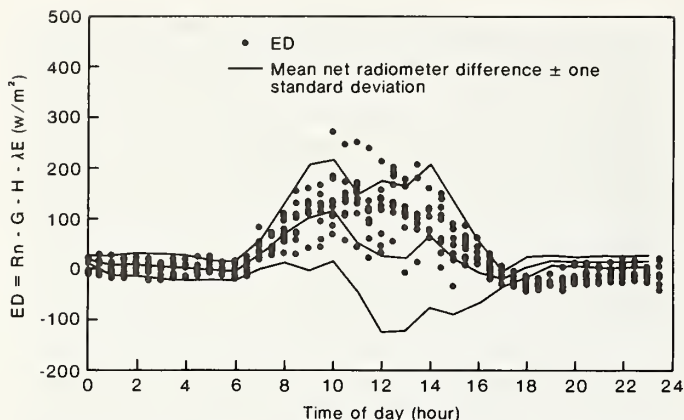


Figure 4.—The 24-hour course of the ED (equation [6] of text) for the 9 days with relatively dry surface conditions in the September 14 to October 31, 1988, data gathering period (data denoted by •). The center solid line gives the mean difference between the two net radiometers for the same set of 9 days. The upper and lower curves are, respectively, the mean plus one standard deviation and the mean minus one standard deviation.

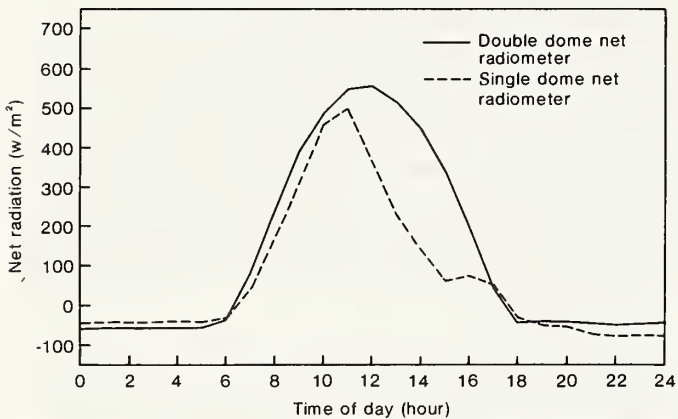


Figure 5.—Comparison of the CPER/LTER net radiometer data with our net radiometer data for September 19, 1988.

calibration offset between the two radiometers. While some of the difference between the two net radiometers is due to the fact that they are positioned over different areas of the Pawnee Grassland surface, such large differences (over 250 w m^{-2}) cannot be explained by surface differences. Furthermore, in a detailed study by Kanemasu (Kanemasu,⁵ Kanemasu et al. 1987) surface differences are small, yet they also found large and systematic differences between different net radiometers, with the double dome net radiometer generally showing the highest values for R_n .

In addition to the radiometer problems, the ED also includes any errors associated with the soil heat flux measurements. Figure 7 gives a comparison of the 24-hour time courses for the two soil heat flux plates for September 19, 1988. The measurements show that there are some small differences (about 10 w m^{-2} to 25 w m^{-2}) between the two heat flux plates, and because ours is buried at a 10-cm depth we can expect it to underestimate the peak magnitudes of G as well as to lag behind G by at least 1 hour or more (Fuchs and Tanner 1968). Had we corrected for soil heat storage in the overlying 10 cm of soil (Fuchs and Tanner 1968), we would have minimized this

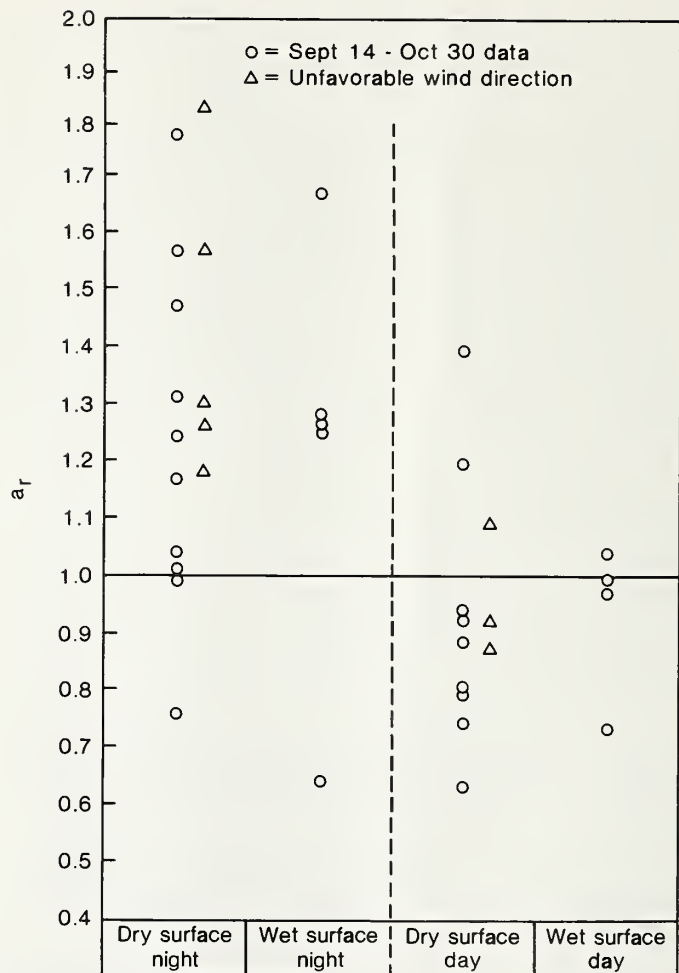


Figure 6.—Performance of the double dome net radiometer relative to the CPER/LTER single dome net radiometer for the September 14 to October 30 data gathering period. Daytime data includes only cloud-free days.

error (which could conceivably increase our measurement of G by a factor of 2 to 3). However, the representativeness of any particular correction for soil heat storage or any particular measurement of G will always be open to question in an area of partial canopy cover such as at the Pawnee Grasslands. It is probably not possible to obtain a representative estimate of G at the Pawnee site without first averaging many different measurements taken throughout the area. In addition to these major corrections and questions about G , Philip (1961) showed that there is also an important correction to G due to the geometry of the sensor. In our case this correction means that the soil heat flux plate is probably underestimating G between 10% and 20%.

From the above discussions and information from other researchers, we recomputed the EBR and ED arbitrarily assuming that the true R_n was 80% of the measured R_n whenever R_n was positive and that it was 150% of the measured R_n whenever R_n was negative and that the true soil heat flux was three times the measured G . Although the above corrections to R_n and G are reasonable, they are not meant to be definitive or precise. They are simply part of a plausibility argument supporting the con-

tention that an overestimation of $R_n - G$ is the major cause for the lack of energy balance closure. Other correction factors are possible, but the ones we have chosen seem quite reasonable and realistic. Figure 8 gives the recomputed ERB values for the 20 days of favorable wind directions and clearly shows much improvement in closure of the energy balance since all ERB values are between 1.1 and 0.83 with most of the 20 daily ERB values quite close to 1.0. Figure 9 shows the 24-hour time course for the recomputed ED for the 20 days of favorable wind direction. This figure shows that the maximum daily ED is substantially reduced (usually to less than about 100 wm^{-3}) and the daily nighttime ED values are generally about -30wm^{-3} . It would appear that the lack of energy balance closure is more likely caused by deficiencies in the measurements of net radiation and soil heat flux than by problems with eddy correlation.

The final comparison we make is between evapotranspiration rates measured with a weighing lysimeter and with the krypton hygrometer-based eddy correlation

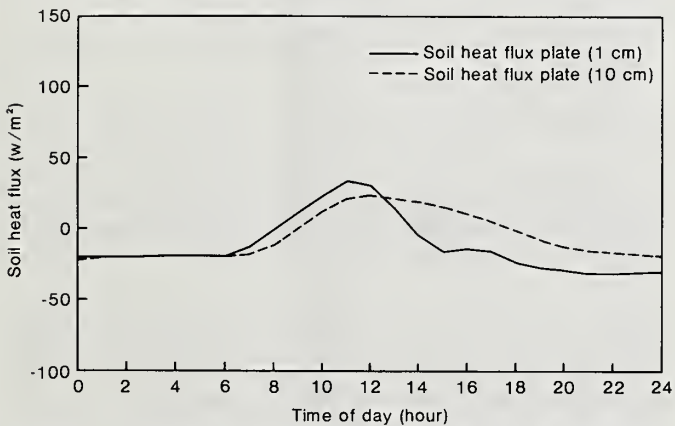


Figure 7.—Comparison of the CPER/LTER soil heat flux plate data with our soil heat flux plate data for September 19, 1988.

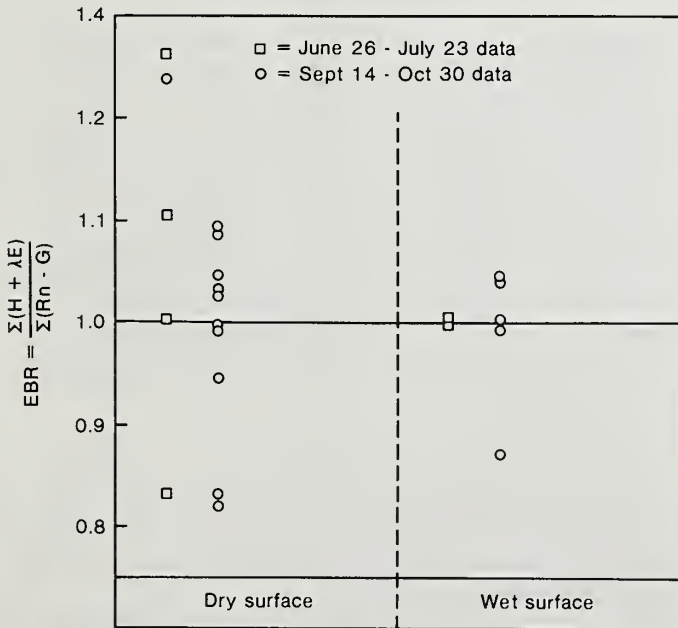


Figure 8.—Same as figure 3 except for corrections to net radiometer and soil heat flux data. See text for further details.

approach. Figure 10 gives the 24-hour time course of evapotranspiration rates for September 19, 1988 as estimated by these two techniques. There are obvious differences from 1 hour to the next, but over the whole day the total water loss is quite similar. However, this 1 day is atypical in the nearly perfect agreement between these two approaches. Generally, as shown in figure 11, the eddy correlation method gives estimates of evapotranspiration which exceed the lysimeter estimates—this corresponds to the region $a_e < 1$ on this figure. Here a_e is the regression coefficient for each 24-hour period for both the wet and dry surface conditions and as such is a daily averaged measure of how one method of estimating evapotranspiration compares to the other method. The coefficient a_e is determined by a least squares method according to the following relationship:

$$(\lambda E)_{\text{lysimeter}} = a_e (\lambda E)_{\text{eddy correlation}}$$

The data for July 8 and September 14, 1988 were excluded from this analysis because of problems with the lysimeter.

This comparison gives further support to the supposition that the lack of closure of the energy balance is not caused by an underestimation of $\lambda E + H$ by eddy correlation; otherwise, we would also have to conclude that the weighing lysimeter is underestimating λE by even

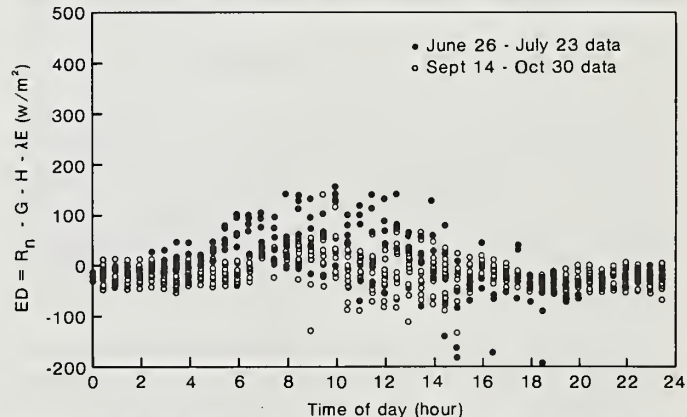


Figure 9.—Same as figure 4 except for the corrections to net radiometer and soil heat flux data and the inclusion of all 20 days of favorable wind direction. See text for further details.

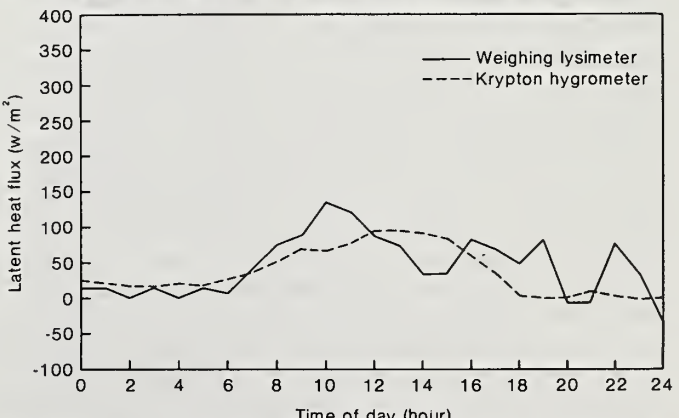


Figure 10.—Comparison of the CPER/LTER weighing lysimeter estimates of evapotranspiration with the eddy correlation estimates of September 19, 1988.

greater amounts which, in turn, would suggest that these lysimeter estimates of λE would probably not be representative of the Pawnee Grasslands.

In general, the relative performances of these two methods do not seem to be much influenced by wet or dry conditions or by the wind blowing across the shelter. On the other hand, the correlation coefficient, a_e , does seem to display a wide range of variation. This could be due, in part, to the fact that the effective evapotranspiring surface sensed by the eddy correlation is significantly larger than that sensed by the lysimeter. The eddy correlation system is, therefore, more likely to be responsive to the heterogeneous distribution of sources of water vapor in an arid ecosystem with partial canopy cover such as the Pawnee Grasslands. It should also be pointed out here that the fact that the coefficient a_e does not show particular sensitivity to whether or not the wind is blowing across the shelter lends support to the hypothesis that sensible heat is removed from the air as it passes over the shelter, thereby reducing the EBR for those days. If a_e had shown sensitivity to whether the wind direction was favorable or unfavorable, then we would have to conclude that the λE component of the energy balance could also be influenced by the site geometry. The results of figure 11 indicate that our shelter is not acting as a significant local source or sink for water vapor because λE is not sensitive to unfavorable wind directions.

Conclusions and Recommendations

In conclusion, we accept the eddy correlation approach for estimating the sensible and latent heat fluxes. Therefore, the same methodology should give reliable estimates of the dry deposition fluxes for ozone, NO_2 , and NO_x , or other trace gases, providing we characterize the errors inherent with the use of any particular instrument or experimental design which will be used for making these measurements.

The lack of energy balance closure is largely caused by errors primarily in the measurements of net radiation and secondarily in soil heat flux measurements. The sensible and latent heat fluxes are likely to correct to within 5% or at most 10% (assuming proper screening of the data for known sources of errors; e.g., Zeller et al. 1989). The available energy ($R_n - G$), on the other hand, can have errors in excess of 30%. The largest unmeasured component of the energy balance is the horizontal flux of sensible and latent heat, D , which, as we have tried to demonstrate, may be quite significant. However, at our site there should not be any serious contamination of the fluxes except when the wind is blowing over the instrument shelter and through the tower. On the other hand, D may still be contributing to our eddy correlation flux measurements, but without greater certainty in the measurements of R_n and G we cannot quantify this potential source of error. It seems likely though that D under favorable wind conditions will be considerably below 100 w/m^2 which we observed to be the approximate magnitude of D during unfavorable wind regimes.

Given the importance of the energy balance to ecosystems and the influence and interactions ecosystems

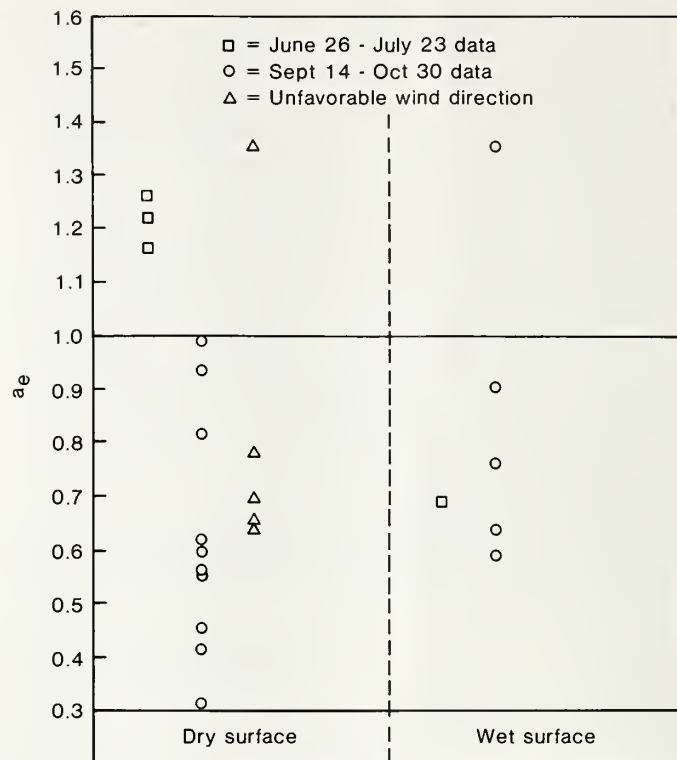


Figure 11.—Performance of the CPER/LTER weighing lysimeter for estimations of evapotranspiration relative to the eddy correlation estimates for 24 of the 26 days listed in table 2.

can have on their ambient environment, a further study of the problems associated with the measurement of the net radiation and soil heat flux is essential.

Literature Cited

- Abramowitz, M.; Stegun, I. E., eds. 1970. Handbook of mathematical functions. National Bureau of Standards Applied Math. Ser. 55. Washington, DC. 1046 p.
- Amrijo, J. D.; Twitchell, G. A.; Burman, R. D.; Nunn, J. R. 1972. A large, undisturbed, weighing lysimeter for grassland studies. Transactions of the American Society of Agricultural Engineers. 15: 827-830.
- Andreas, E. L. 1981. The effects of volume averaging on spectra measured with a Lyman-Alpha hygrometer. Journal of Applied Meteorology. 20: 467-475.
- Brown, L. F.; Trlica, M. J. 1977. Carbon dioxide exchange of blue grama swards as influenced by several ecological variables in the field. Journal of Applied Ecology. 14: 205-213.
- Conklin, P. S.; Knoerr, K. R.; Schneider, T. W.; Baker, C. B. 1988. In: Eighth symposium on turbulence and diffusion; 1988 April 26-29; San Diego, CA. Boston, MA. American Meteorological Society. A wind tunnel test of probe shadow effects on a sonic anemometer in two orientations: 108-111.
- Fuchs, M.; Tanner, C. B. 1968. Calibration and field test of soil heat flux plates. Soil Science Society of America Proceedings. 32: 326-328.

Henderson-Sellers, B. 1984. A new formula for heat of vaporization of water as a function of temperature. *Quarterly Journal of the Royal Meteorological Society*. 110: 1186–1190.

Kaimal, J. C.; Wyngaard, J. C.; Haugen, D. A. 1968. Deriving power spectra from a three-component sonic anemometer. *Journal of Applied Meteorology*. 7: 563–589.

Kanemasu, E. T.; Asar, G.; Nie, D.; Watts, D.; Fritschen, L.; Gay, L.; Weaver, H.; Stannard, D.; Tanner, B.; Tanner, M.; Green, J. 1988. In: *Flow and transport in the natural environment: advances and applications; 1987 31 August–4 September; Canberra, Australia*. Canberra, ACT Australia. Australian Academy of Science: Inter- and Intra-sensor comparison among Bowen ratio and eddy correlation instruments.

McCaughey, J. H.; Saxton, W. L. 1988. Energy balance storage terms in a mixed forest. *Agricultural and Forest Meteorology*. 44: 1–18.

McMillen, R. T. 1986. A basic program for eddy correlation in non-simple terrain. NOAA Tech. Memo ERL ARL-147 ATDD. Oak Ridge, TN: National Oceanic and Atmospheric Administration. 32 p.

Moore, C. J. 1986a. Estimating heat storage in Amazonian tropical forest. 1986. *Agricultural and Forest Meteorology*. 38: 147–169.

Moore, C. J. 1986b. Frequency response corrections for eddy correlation systems. *Boundary-Layer Meteorology*. 37: 17–35.

Otnes, R. K.; Enochson, L. 1978. *Applied time series analysis. Vol. I, basic principles*. New York, NY: John Wiley and Sons, Inc. 449 p.

Philip, J. R. 1961. The theory of heat flux meters. *Journal of Geophysical Research*. 66: 571–579.

Tanner, B. D. 1988. Use requirements for Bowen Ratio and eddy correlation determination of evapotranspiration. Paper presented at the 1988 Speciality Conference of the Irrigation and Drainage Division of the American Society of Civil Engineers. Lincoln, NB.

Tanner, B. D.; Greene, J. P. 1989. Measurement of sensible heat and water vapor fluxes using eddy correlation methods. Final Report, Campbell Scientific Contract No. DAA09-87-D-0038 to U.S. Army Dugway Proving Grounds. Salt Lake City, UT: Campbell Scientific. 17 p.

Webb, E. K.; Pearman, G. I.; Leunig, R. 1980. Correction of flux measurements for density effects due to heat and vapor transfer. *Quarterly Journal of the Royal Meteorology Society*. 106: 85–100.

Weeks, E. P.; Weaver, H. L.; Campbell, G. S.; Tanner, B. D. 1987. Water use by salt cedar and by replacement vegetation in the Pecos River floodplain between Acme and Artesia, New Mexico. U.S. Geological Survey Professional Paper 491-G. Washington, DC: U.S. Government Printing Office. 33 p.

Wesely, M. L. 1988. Use of variance techniques to measure dry air-surface exchange rates. *Boundary-Layer Meteorology*. 44: 13–31.

Wyngaard, J. C.; Zhang, S. 1985. Transducer-shadow effects on turbulence spectra measured by sonic anemometers. *Journal of Atmospheric and Oceanic Technology*. 2: 548–558.

Zeller, Karl; Massman, William; Stocker, David; Fox, Douglas G.; Stedman, Donald; Hazlett, Donald. 1989. Initial results from the Pawnee eddy correlation system for dry acid deposition research. Res. Pap. RM-282. Fort Collins, CO: U.S. Department of Agriculture, Forest Service, Rocky Mountain Forest and Range Experiment Station. 30 p.

Zhang, S.; Wyngaard, J. C.; Businger, J. A.; Oncley, S. P. 1986. Response characteristics of the U.W. sonic anemometer. *Journal of Atmospheric and Oceanic Technology*. 3: 315–323.

Appendix A

Sonic Anemometer Shadowing Algorithm

Shadowing, common to virtually all sonic anemometers (Wyngaard and Zhang 1985, Zhang et al. 1986), refers to the underestimation of the ambient wind velocity caused by the anemometer transducer wakes along the acoustic paths. In this appendix we give the details of the algorithm we use for correcting the 3-axis sonic anemometer used in this study.

We deploy the 3-axis sonic in the rotated position (Conklin et al. 1988) with two transducer axes in the horizontal plane and the third in the vertical direction. We developed the algorithm from the wind tunnel data generously provided by Paul Conklin.⁶ Figure A-1 gives the horizontal geometry used for the algorithm. Since we treat the horizontal and vertical corrections as independent, we begin with the correction algorithm for the horizontal components of the wind velocity.

Figure A-2 gives the u components shadowing data as a ratio of the wind tunnel's u wind speed to the sonic's measured u wind speed. However, these data are not exactly the same as Conklin's data. First, we required the original data to be consistent with the symmetry of the sonic's design. Next we averaged the symmetrized re-

⁶Conklin 1988 – personal communication.

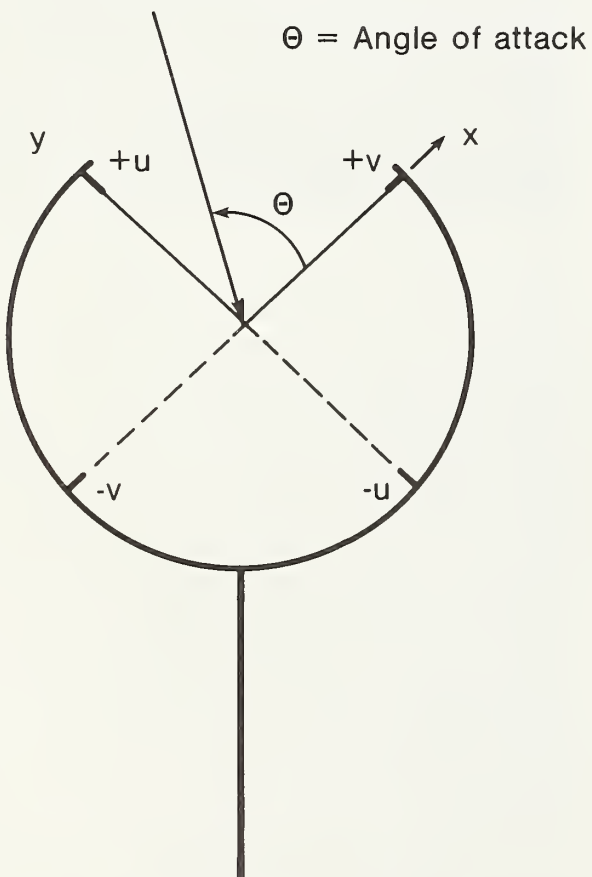


Figure A-1.—Geometry of the horizontal components of the 3-axis sonic anemometer.

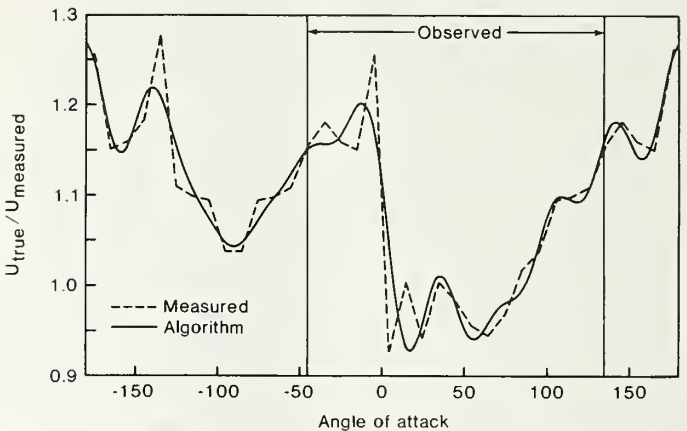


Figure A-2.—Shadowing effects of the u transducer component of the 3-axis sonic anemometer.

sponses of the u and v components after first removing what appeared to be dubious and/or asymmetric data points. Finally, we extended the original data set (again using symmetry arguments) into the region where no data had originally been gathered. This extension does, however, introduce some uncertainty into the shadowing correction when it is applied in the region outside of the original data are relatively minor, introducing an error estimated to be no greater than 5%; however, they aid completely symmetric under rotation about an axis of symmetry between the two sensors. These changes to the original data are relatively minor introducing an error estimated to be no greater than 5%; however, they aid enormously in the development of the algorithm. Finally, it should be emphasized that shadowing effects can be quite significant since they can introduce errors greater than 25% depending upon the angle of attack. For accurate measurements of Reynolds stresses, shadowing corrections can become extremely important.

Also given in figure A-2 is the analytical representation of the extended and symmetrized data set which is used for the algorithm. This analytical representation was derived from a fast Fourier transform of this data and then reconstructed from the mean and the first 10 harmonics. It is necessary to keep all these higher harmonics because the nearly discontinuous response near $\theta = 0$ cannot be represented with fewer than 10 harmonics. However, for designing the algorithm we did not employ the Fourier basis functions, $(\sin(n\theta) \text{ and } \cos(n\theta))$, rather we transformed into a system defined by the following basis functions, $\sin(\theta)\cos^{n-1}(\theta)$ and $\cos^n(\theta)$. The relationship between the two sets of basis functions is defined as follows:

$$\begin{aligned} \cos(n\theta) &= T_n(\cos(\theta)) \\ \sin(n\theta) &= \sin(\theta) U_{n-1}(\cos(\theta)) \end{aligned}$$

where T_n and U_{n-1} are Chebyshev polynomials (Abramowitz and Stegun 1970). To produce the v component correction we followed the same procedure, and the data we used are the same as that given in figure A-2 except that the angle of attack is replaced by its complement. This gives rise to a different set of Fourier coefficients and hence the need to correct the u and v components separately.

For the vertical component the analysis is considerably simpler. In part, this is because the attack angle of the wind relative to the vertical axis is generally restricted to only a few degrees above or below the horizontal plane, i.e., $w < < u, v$. Conklin's data are limited to about 12 degrees off true horizontal, and we found no strong angular dependence due to shadowing; therefore, we simply took the average of his data for the vertical sensor after ensuring that the vertical correction was consistent with the horizontal data with similar attack angles. This led to a constant correction factor for the vertical sonic path of 1.16 as quoted in the main body of the text. In a concurrent analysis of these data Baker⁷ derived a value of 1.18 for the vertical correction which agrees quite well with our results. The present real time on-line algorithm is given as follows:

```

r2 = x*x + y*y
if(r2 .lt. 00001) return
sqr2i = 1./sqrt(r2)
s1 = y*sqr2i
c1 = x*sqr2i
c2 = c1*c1
s2 = s1*c1
c3 = c2*c1
s3 = s2*c1
c4 = c2*c2
s4 = s2*c2
c8 = c4*c4
s8 = s4*c4
u1 = -0.149833*c1 - 0.012816*s1
u2 = 0.634013*c2 - 0.164306*s2
u3 = 0.796858*c3 + 0.006149*s3
u4 = -4.594717*c4 + 0.902447*s4
u5 = (-3.101117*c1 - 1.549559*s1)*c4
u6 = (15.123799*c2 - 3.549725*s2)*c4
u7 = (4.666539*c3 + 3.935484*s3)*c4
u8 = -19.795181*c8 + 6.192350*s8
u9 = (-2.294395*c1 - 2.762220*s1)*c8
u10 = (8.787828*c2 - 3.822010*s2)*c8
u = (1.11178+u1+u2+u3+u4+u5+u6+u7
     +u8+u9+u10)*y
v1 = -0.382962*c1 - 0.081949*s1
v2 = -1.574396*c2 - 0.441242*s2
v3 = 2.335394*c3 + 0.583344*s3
v4 = 9.883878*c4 + 2.907992*s4
v5 = (-6.316420*c1 - 2.867878*s1)*c4
v6 = (-23.821350*c2 - 7.904744*s2)*c4
v7 = (7.113387*c3 + 4.511051*s3)*c4
v8 = 24.143967*c8 + 9.095705*s8
v9 = (-2.762217*c1 - 2.294400*s1)*c8
v10 = (-8.787828*c2 - 3.822010*s2)*c8
v = (1.26752+v1+v2+v3+v4+v5+v6+v7
     +v8+v9+v10)*x
w = 1.16*z

```

where x, y, and, z are the uncorrected sonic u, v, and w measurements, respectively.

For flux measurements only the vertical correction is necessary which is particularly simple to apply after the data have been gathered. However, it is important to use

⁷Baker 1988 – personal communication.

this algorithm in real time to minimize errors in the Reynolds stresses which may result from shadowing.

Finally we wish to emphasize that this algorithm is tentative and undergoing testing. It was derived for only one wind speed (3 ms^{-1}) and, hence, may require redesign when further tests are performed. A more extensive data set covering a greater range of attack angles and wind speeds may suggest a better set of basis functions for the analytical development as well as indicate any influence wind speed may have on the shadowing. Furthermore, more data is required to verify some of the extensions and symmetry arguments on which this algorithm is based.

Appendix B

Correction of Krypton Hygrometer for O₂ Effect

This appendix is an adaptation of the work of Tanner (henceforth denoted by T89) for correcting the krypton hygrometer data for influence that oxygen can have upon the fluctuating component of the water vapor density, ρ'_v .

Without repeating the details provided in T89, we will write his equation [10] as follows:

$$\rho'_v = (\rho'_v)_m + \rho\beta T'/T \quad [B-1]$$

where β is a constant ($\beta = 0.0131 \pm 0.0018$ and is derived from T89), $(\rho'_v)_m$ is the measured water vapor density, and all other symbols are as defined in the text. The uncertainty of ± 0.0018 in β is a result of natural variation in the adsorption coefficient for water vapor (T89). For our site $\rho = 1.0 \text{ kgm}^{-3}$ and, therefore, we obtain by multiplication the value of $\alpha = \rho\beta$ given in equation [3] of the main text. Following T89 we derive equation [3] of the text by taking the correlation between the terms of equation [B-1] and w' .

For our eddy correlation system we can correct the vapor flux at the end of every half-hour by a straightforward application of equation [3]. However, for correcting the variance of water vapor density, either equation [B-1] can be used each time a new measurement of the water vapor density, $(\rho'_v)_m$, is made or the method suggested by Tanner and Greene (1989) could be employed. The first method requires the computations to be done on line in real time at eddy flux correlation data rates by the computer data processing software (McMillen 1986, Zeller et al. 1989). The second method requires computing the correlation, $(\rho'_v)_m T'$, for every half-hour. However, this second approach also requires correcting for sensor separation and sensor inadequacies (Wesley 1988).

Appendix C

Transfer Function for Krypton Hygrometer

In this appendix, we provide the spectral transfer function for the volume averaging effects of the krypton hygrometer. We use this function to model the hygrometer performance when estimating the corrections arising

from inadequate instrument response as shown in figures 1 and 2 of the main text and as discussed in detail in appendix B of Zeller et al. (1989). The main limitation of fast response hygrometers largely results from the fact that any measurement of the turbulent fluctuations of water vapor density, ρ'_v , actually represents an average over the volume bounded by the right circular cylinder defined by the hygrometer windows rather than a true point measurement (Andreas 1981).

Following the methods detailed in Zeller et al. (1989) and employing their notation, the results of Andreas (1981) are given as follows:

$$T_h(n) = \frac{640}{3\pi(k_l l)^4(d)^2} \int_0^\infty dx_2 dx_3 \left[\frac{\sin(x_3 k_l l/2)}{x_3} \right]^2 \left[\frac{J_1^2(k_l l(d/l)) (1+x_2^2)^{1/2}/2}{(1+x_2^2)(1+x_2^2+x_3^2)^{1/6}} \right]^2 \quad [C-1]$$

where $k_l = 2\pi/u$ with n being spectral frequency and u is the mean horizontal wind speed, l is the hygrometer path length ($l = 0.987$ cm for our hygrometer), d is the diameter of the hygrometer windows ($d = 1.961$ cm for our hygrometer), and J_1 is a Bessel function. Figure C-1 gives T_h as a function of $k_l l$ for our krypton hygrometer which has an aspect ratio, d/l , equal to 2.0.

Appendix D

A Digital Anti-Aliasing Filter

The purpose of this appendix is to present a digital version of the Butterworth filter which can be used in real time for eddy correlation. The main utility of these

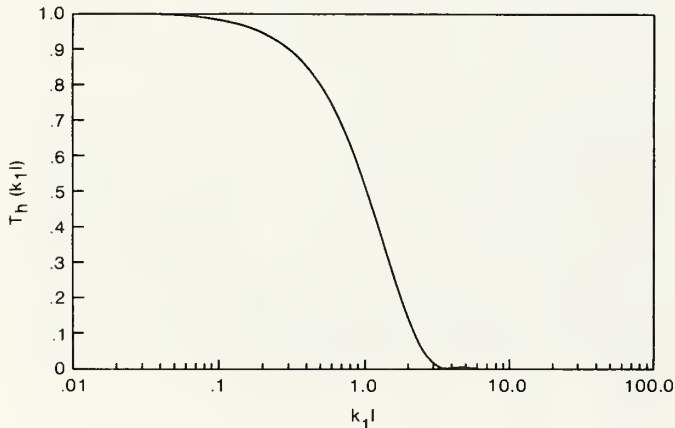


Figure C-1.—Spectral response function, $T_h(k_l l)$, associated with the volume averaging of the fluctuations of water vapor density by the krypton hygrometer.

low pass filters is to reduce aliasing of spurious, high frequency, electronic noise and the aliasing of naturally occurring frequencies which are higher than the sampling frequency. The present digital filter is an alternative to the more commonly used analog filter designed as an electronic circuit (Moore 1986b). Zeller et al. (1989) give more detail on the Butterworth filter.

The response function for the analog form of a 2-pole low pass Butterworth is given as follows:

$$T_B(n) = (1+(n/n_0)^4)^{-1/2} \quad [D-1]$$

where n_0 is the Nyquist frequency equal to one-half the sampling frequency, n_s . Here we are assuming that the cutoff frequency is n_0 , whereas the 2-pole digital filter developed here has a slightly different form:

$$T_B(n) = (1+\tan^4(\pi n/n_s)/\tan^4(\pi n_c/n_s))^{-1} \quad [D-2]$$

where n is frequency and n_c is defined as the cutoff frequency, which we will take to be $n_s/4$. This particular cutoff frequency simplifies equation [D-2] since $\tan(\pi n_c/n_s) = 1$.

For the purposes of estimating the corrections due to sensor inadequacies, the form given by equation [D-2] above is not the best for numerical evaluation. We use the following equivalent representation:

$$T_B(n) = 4\cos^4(\pi n/n_s)/(3 + \cos(4\pi n/n_s)) \quad [D-3]$$

The main difference between these two forms of the Butterworth filter is the lower cutoff frequency of the digital filter and the concomitant loss of information at somewhat lower frequencies than would occur with the analog version. However, at our present sampling rates of 20 to 40 Hz, this loss is not significant. Furthermore, it can easily be accounted for by the method outlined by Zeller et al. (1989) for correcting the eddy correlation fluxes.

Using the methods outlined in Otnes and Enochson (1978) it is straightforward to calculate the poles and zeroes of equation [D-2] and to derive the following recursive digital filter which is the equivalent of equation [D-2]:

$$q'(i) = 0.085786438q(i) + 0.343145751q(i-1) + 0.514718626q(i-2) + 0.343145751q(i-3) + 0.085786438q(i-4) - 0.343145751q'(i-2) - 0.029437252q'(i-4)$$

where $q(i)$ and $q'(i)$ represent, respectively, the most recent real time estimate of the mean and fluctuating components of the atmospheric quantity being measured and the $i-1$ index refers to the immediately previous estimate of those quantities and so forth until $i-4$. This recursive filter is applied in the manner similar to the recursive filter discussed by McMillen (1986). We have tested this filter and found that it reduces the heat flux measurement with our eddy correlation system by about 3%.

Massman, W. J.; Fox, D. G.; Zeller, K. F.; Lukens, D. 1990. Verifying eddy correlation measurements of dry deposition: a study of the energy balance components of the Pawnee Grasslands. Res. Pap. RM-288. Fort Collins, CO: U.S. Department of Agriculture Forest Service, Rocky Mountain Forest and Range Experiment Station. 14 p.

The surface energy balance is used to assess the performance of the Pawnee Grasslands eddy correlation system. The four major components of the energy balance were measured: the net radiation, R_n ; the soil heat flux, G ; and the sensible and latent heat fluxes, H and λE , respectively. The latter two components were measured by eddy correlation. The surface energy balance defined as, $R_n - G = H + \lambda E$, was not achieved, most likely because measurements of R_n and G were not adequate.

Keywords: Eddy correlation, Pawnee Grasslands, surface energy balance closure, latent heat flux, sensible heat flux, net radiation, soil heat flux



Rocky
Mountains



Southwest



Great
Plains

U.S. Department of Agriculture
Forest Service

Rocky Mountain Forest and Range Experiment Station

The Rocky Mountain Station is one of eight regional experiment stations, plus the Forest Products Laboratory and the Washington Office Staff, that make up the Forest Service research organization.

RESEARCH FOCUS

Research programs at the Rocky Mountain Station are coordinated with area universities and with other institutions. Many studies are conducted on a cooperative basis to accelerate solutions to problems involving range, water, wildlife and fish habitat, human and community development, timber, recreation, protection, and multiresource evaluation.

RESEARCH LOCATIONS

Research Work Units of the Rocky Mountain Station are operated in cooperation with universities in the following cities:

Albuquerque, New Mexico
Flagstaff, Arizona
Fort Collins, Colorado *
Laramie, Wyoming
Lincoln, Nebraska
Rapid City, South Dakota
Tempe, Arizona

*Station Headquarters: 240 W. Prospect Rd., Fort Collins, CO 80526